

# LATERAL DIFFUSION AND PHASE SEPARATION IN TWO-DIMENSIONAL SOLUTIONS OF POLYMERIZED BUTADIENE LIPID IN DIMYRISTOYLPHOSPHATIDYLCHOLINE BILAYERS

## A Photobleaching and Freeze Fracture Study

H. GAUB AND E. SACKMANN

*Physics Department of Technical University of München, 8046 Garching bei München, Federal Republic of Germany*

R. BÜSCHL AND H. RINGSDORF

*Institute of Organic Chemistry, Johannes-Gutenberg University of Mainz, 6500 Mainz, Federal Republic of Germany*

**ABSTRACT** Mixed vesicles of dimyristoylphosphatidylcholine (DMPC) and a polymerizable lipid containing one diene group per chain are studied by freeze fracture electron microscopy and by the photobleaching (fluorescence recovery after photobleaching) technique. Large thin-walled vesicles of some micron in diameter become more stable after photochemical polymerization. Before polymerization bilayers of the diene lipid exhibit a liquid crystal-to-gel transition at  $T_g = 31^\circ\text{C}$ . Upon polymerization the transition remains but shifts to a slightly higher temperature ( $T_g^* = 34^\circ\text{C}$ ). The transitions in both cases are accompanied by a freezing in of the lateral mobilities. The mixed vesicle exhibits lateral phase separation after polymerization. Before polymerization the two lipids appear miscible at all compositions in the fluid state and at DMPC concentrations at or below 50 mol % in the solid state. After polymerization a two-dimensional solution of the polymer in DMPC is obtained at  $T > T_g^*$ , while lateral phase segregation into DMPC-rich domains and patches of the polymer is observed at  $T < T_g^*$ . The domain structure appears identical irrespective of whether polymerization is performed at  $T > T_g$  or at  $T < T_g$ . A typical value of the diameter of the polymerized lipid domains ( $\sim 400$  Å) indicates a rather small aggregation number ( $N < 100$  monomers). The lateral diffusion coefficient in butadiene-lipid bilayers only decreases from  $D_1 = 3 \cdot 10^{-7} \text{ cm}^2/\text{s}$  to  $D_1 = 8 \cdot 10^{-8} \text{ cm}^2/\text{s}$  (that is by a factor of 4) upon polymerization. This is consistent with the freeze fracture finding of a small aggregation number. We point out the similarities of the mixed vesicles with plasma membranes coupled to the cytoskeleton.

### INTRODUCTION

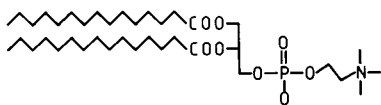
Lipid bilayers are fascinating not only because of their essential role as basic building units of biological membranes but also because they provide model systems with which to study the physical properties of two-dimensional systems. In recent years the interest in lipid vesicles has also been stimulated by the hope that these systems would provide interesting applications, either technologically or as drug carrier systems (1–3). Recently the preparation of polymerizable lipids (3–7) has opened up the possibility of preparing more stable vesicles. By using mixtures of polymerized and nonpolymerized lipids, it is simultaneously possible to control the selective opening of the membrane (8) or to prepare giant vesicles that can undergo fusion into still larger systems by dielectric breakdown (9). Further-

more, these mixtures are expected to have viscoelastic properties which are analogous to those of plasma membranes, and to provide interesting model systems of two-dimensional polymer solutions to test theories of scaling laws (10).

Large vesicles of a binary mixture of a polymerizable butadiene lipid (Scheme I) and dimyristoylphosphatidylcholine (DMPC, Scheme II) were studied by photobleaching using the dye diO<sub>18</sub> (Scheme III) as molecular probe and by freeze fracture electron microscopy.

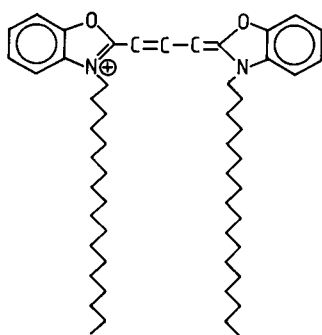


Scheme I



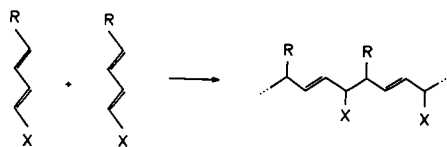
Scheme II

Each molecule of butadiene lipid (Scheme I) can cross-link with up to four neighbors so that two-dimensional networks may be formed. In contrast to the diacetylenic lipids (3–6), the polymerization of butadiene carrying lipids is nontopochemical and cross-linking can be effected both in the fluid and the crystalline phase. The photochemical polymerization by irradiation most probably leads to the following structure, Scheme IV (11, 12)



Scheme III

The lateral diffusion coefficient of the diO<sub>18</sub> probe was measured by the photobleaching (fluorescence recovery after photobleaching, FRAP) technique to study the molecular transport properties in such systems and to get information about the molecular weight and the degree of cross-linking (branching) of the polymer. Electron microscopy provides information about the microscopic organization of the mixed bilayers at temperatures where at least one or both of the two lipid components are in the solid state.



Scheme IV

## MATERIALS AND METHODS

### Materials

The polymerizable lipid (Scheme I) was prepared as follows 50 mmol of octadecadienoic acid (11) as esterified with 25 mmol *N*-methyliminodiol in the presence of 100 mg dimethylaminopyridine and 65 mmol of dicyclohexylcarbodiimide was added drop by drop (solvent: absolute chloroform). After one day of stirring, the product was isolated by

extraction and recrystallization (yield: 85%).

Quaternization of this methyl-bis (2-octadeca-2,4-dienoyloxyethyl)amine was carried out in acetone by adding an excess of methylbromide. The purity of the product (dimethyl-bis[2-octadeca-2,4-dienoyloxyethyl] ammonium-bromide, yield: 75%) was checked by thin layer chromatography, infrared spectroscopy, NMR, mass spectroscopy, and element analysis. They were all in full agreement with the above mentioned structure.

In the unpolymerized state lipid (Scheme I) swells above 43°C and the fully hydrated bilayers exhibit a fluid-to-solid transition at  $T = 31^\circ\text{C}$ . DMPC was a commercial product (Fluka, A. G., Buchs, Switzerland) and was used without further purification. The  $P'_\beta \rightarrow L_\alpha$  (solid-fluid or main transition) and the  $P'_\beta \rightarrow L'_\beta$  (solid-solid or pretransition) transition temperatures have the usual values  $T_m = 23^\circ\text{C}$  and  $T_p = 15^\circ\text{C}$ , respectively.

## Methods

For the freeze fracture preparation, the lipid was dissolved in chloroform deposited on the wall of a glass flask by solvent evaporation and was taken up at 45°C by 2 ml of water, purified by Millipore filtration. The polymerization was performed by irradiating the vesicle suspension, kept in a quartz cuvette, with a Pen-Ray-UV-lamp (A. R. Vetter Co., Rebersburg, PA) at 254 nm. ~20  $\mu\text{l}$  of vesicle suspension was then sandwiched between gold plates (100  $\mu\text{m}$  thickness, 5 mm diam) and stored at a preselected temperature for 10 min. Then the samples were rapidly cooled by dipping into freon kept at  $T = -160^\circ\text{C}$ . Freeze fracture was performed in a Balzers BAF 400 D device (Balzers, Hudson, NH). Platinum/carbon shadowing was performed under an angle of incidence of 45°C. The electron micrographs were taken in a Philips EM 400 microscope (Philips Electronic Instruments, Inc., Mahwah, NJ).

The FRAP experiments were performed with a modified Zeiss-Axiomat microscope (Carl Zeiss, Inc., Thornwood, NY). A schematic design is given in Fig. 1. The beam of an Argon ion laser (164-09; Spectra-Physics Inc., Mountain View, CA) passes the mirror system (A) of the microscope and is focused on the surface of the light pipe (G). The output is projected by  $L_2$  and a selectively reflecting mirror onto the entrance pupil of the objective. In this way an image of the excited plane of the light pipe is formed on the membrane's surface. The light pipe is mechanically agitated by an electromagnet to smooth down the speckle pattern caused by the coherence of the laser output. This occurs by mixing many speckle pictures with a frequency above the timescale of interest. The recovering fluorescence light passes an interference filter (maximum 520 nm for diO<sub>18</sub> probe). The recording unit consists of a RCA/C31034 photomultiplier (RCA Electro-Optics and Devices, RCA Solid State Div., Lancaster, PA) photon counter (9301/2; Ortec Inc., Oak Ridge, TN) and an Apple microcomputer (Apple Computer Inc., Cupertino, CA). The

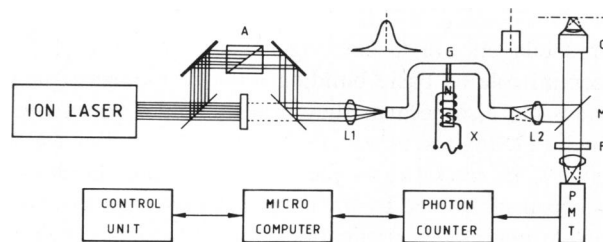


FIGURE 1 Schematic design of photobleaching apparatus. The beam of the Ar-ion laser is focused through an attenuating mirror system (A) on to the surface of the light pipe (G). The outgoing light is projected by a 50% reflecting mirror to the objective (O). A picture of the excited plane of the light pipe is thus imaged on the membrane. The fluorescence light is monitored through an interference filter. An electromagnet (X) is used for mechanical agitation of the light pipe to smear out the speckle pattern of the laser light, which would lead to inhomogeneous bleaching.

control unit serves to drive the shutters of the beam attenuator and the photomultiplier.

One main purpose of the light pipe is to transform the Gaussian intensity profile of the laser into a rectangular profile. This was verified in separate experiments. The main advantage of a rectangular intensity distribution is that the shape of the recovery curve does not depend on the degree of bleaching (13–15). Moreover, the bleaching and illuminating spots have identical profiles and position in the object plane. A disadvantage is that the minimum size of the bleaching spot and the accuracy of the initial slope of the recovery curve are limited by the microscope diffraction.

In our previously used technique (15) a nearly rectangular profile was achieved by cutting off the wings of the laser beam by a small aperture. However, this implies a great loss in intensity. By using the light pipe the full intensity of the laser becomes available. The size of the bleaching spot can be controlled either by using light pipes of variable diameter or by using variable lenses,  $L_2$ . For the present measurements a 25- $\mu\text{m}$  light pipe was used. The bleaching spot had a diameter of 7.14  $\mu\text{m}$ . The vesicles were prepared by swelling the lipid between a microslide and a cover glass in distilled water. The lipid mixture containing appropriate amounts of fluorescence probe was deposited on the microslide by solvent evaporation. Large thin-walled vesicles formed spontaneously after swelling for several minutes at 40–50°C. They remained stable for hours, provided mechanical agitation was avoided. In every case, the photochemical polymerization was performed just before the bleaching experiment.

## RESULTS

Fig. 2 shows the temperature dependencies of the lateral diffusion coefficient,  $D_l$ , of diO<sub>18</sub> in bilayers of butadiene lipid (Scheme I) as well as mixtures of butadiene lipid with DMPC both before and after polymerization. The vesicles of pure DMPC or monomeric butadiene lipid exhibit abrupt changes in  $D_l$ , which characterize their respective

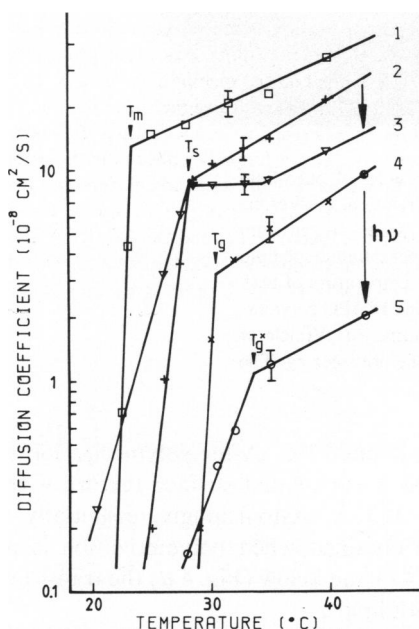


FIGURE 2 Temperature dependence of diffusion coefficient of fluorescence probe diO<sub>18</sub> (Scheme III) in large vesicles of DMPC, butadiene lipid (Scheme I) as well as mixtures of these lipids. Curve 1, pure DMPC; curve 2, 1:1 mixture of DMPC with butadiene lipid before polymerization; curve 3, same mixture after polymerization; curve 4, monomeric butadiene lipid; curve 5, same lipid after polymerization.

transition temperatures. After polymerization of butadiene lipid one still observes a break (at  $T = 34^\circ\text{C}$ ) in the  $D_l$  vs.  $T$  plot indicating a conformational change. Compared with the monomer, this transition is shifted to higher temperatures and considerably broadened. Above the transition temperature, the slope of the  $D_l$ - $T$  curve agrees well with that observed for monomeric butadiene lipid and DMPC.

The mixtures exhibit a more complicated variation of  $D_l$  with a temperature that indicates lateral phase separation. The temperatures where breaks of the  $D_l$  vs.  $T$  plots are observed define the phase boundaries of the mixtures. Consider curve 2 and 3 of Fig. 2. In the unpolymerized state the break at  $28^\circ\text{C}$  defines the liquidus line of the mixture. After polymerization an additional break occurs at  $35^\circ\text{C}$  where the pure polymerized butadiene lipid exhibits a conformational change. The corresponding temperature defines the liquidus line of the two-dimensional solution of the polymerized lipid in DMPC. At lower temperatures separation occurs into a rigid phase that contains mainly polymerized lipid and a fluid DMPC-rich phase. Fast diffusion is still possible in the latter, which results in the horizontal slope of the  $D_l$ - $T$  plot.

In a pure lipid  $D_l$  would decrease with  $T$ , as in curve 1. However, a horizontal deflection is expected since with decreasing temperature polymerized lipid is continuously excluded from the DMPC-rich regions which leads to an increase in the average mobility. Fig. 3 shows the variation of the diffusion coefficient during the process of polymerization for different compositions. In pure butadiene lipid (Scheme I) the process is essentially completed after  $\sim 60$  s. By using thin layer chromatography, it was shown in a separate experiment that the fraction of free monomer is smaller than 10% after 60 s. With increasing DMPC content the half-life time of the polymerization reaction is clearly much longer.

In Fig. 4 some examples of the vesicles' microstructure are presented. Fig. 4a shows a vesicle of pure lipid

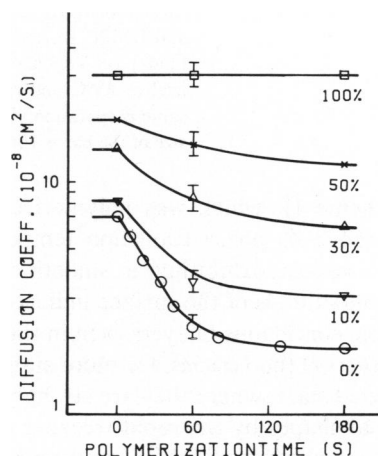


FIGURE 3 Variation of diffusion coefficient,  $D_l$ , of mixtures of DMPC and butadiene lipid with polymerization time. The numbers indicate mole fractions of DMPC.

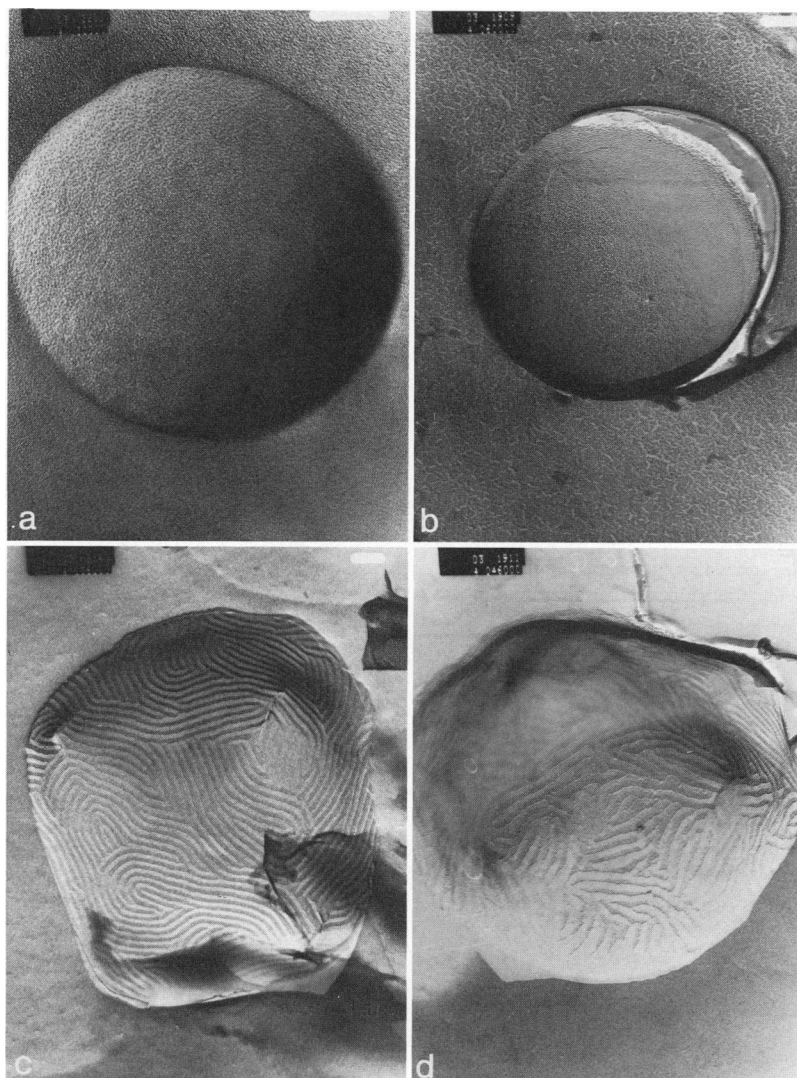


FIGURE 4 Freeze fracture micrographs of giant vesicles of pure lipid and of mixture with DMPC before and after polymerization. (a) Vesicle of pure lipid (butadiene) polymerized at 43°C and rapidly frozen from this temperature. (b) Vesicle of 1:1 mixture of monomeric butadiene lipid and DMPC frozen from 17°C (below the transition temperature of both lipids). (c) Vesicle of 1:1 mixture of butadiene lipid and DMPC polymerized at 43°C and rapidly frozen from this temperature. (d) Vesicle of same preparation after polymerization at  $T = 17^{\circ}\text{C}$  before freezing. The size of the bar is 100 nm.

(butadiene; Scheme I), which was polymerized at  $T = 43^{\circ}\text{C}$ , that is above its phase transition temperature. A large spherical vesicle exhibiting a smooth surface is observed. The smoothness of the surface indicates that the lipid forms stable continuous bilayers even in the polymerized state. Moreover, the vesicles are more stable than in the unpolymerized state, where they are strongly distorted into nonspherical shapes by the rapid freezing procedure. Vesicles of the 1:1 mixture of DMPC and unpolymerized butadiene lipid exhibit smooth surfaces both above ( $T = 43^{\circ}\text{C}$ ) and below ( $T = 23^{\circ}\text{C}$ ) the transition temperatures of the two pure components. Fig. 4 *b* shows the vesicle

when frozen from 17°C. After polymerization the mixed vesicles show a corrugated surface texture with a wavelength of  $\sim 390 \text{ \AA}$ . Astonishingly, essentially the same structure is obtained when polymerization is performed above (Fig. 4 *c*) and below (Fig. 4 *d*) the transition temperatures of both lipids.

#### DISCUSSION

The butadiene lipid (Scheme I) forms stable vesicles both in the unpolymerized and in the polymerized state. Judged from the freeze fracture electron microscopy studies, large

vesicles are more stable if the lipid is polymerized. Each lipid molecule has two polymerizable groups that allow the formation of a branched two-dimensional network or gel. According to Fig. 2, the lateral mobility of the fluorescence probe is frozen at  $T_g = 31^\circ\text{C}$  for the unpolymerized and at  $T_g^* = 34^\circ\text{C}$  for the polymerized butadiene lipid. In a separate experiment it was shown that the rotational mobility of a diphenylhexatriene (DPH) probe is reduced at about the same temperatures. On the other hand a sharp thermotropic transition of the unpolymerized lipid (butadiene) is observed by calorimetry at a lower transition temperature (R. Büschl, unpublished observations). This transition vanishes upon polymerization.

Both transitions can, however, be seen in densitometric measurements (H. Gaub, unpublished observations). The lower transition exhibits a sharp drop in molecular volume characteristic of a chain melting phase change. In accordance with calorimetry, the upper transition is characterized by a break in the density vs. temperature plot at  $T_g = 30^\circ\text{C}$  for the unpolymerized and  $T_g^* = 35^\circ\text{C}$  for the polymerized lipid (butadiene). Clearly, the upper conformational change is not a typical chain melting transition and is not suppressed by polymerization. More experiments are necessary to clarify the structural changes at this second-orderlike phase change that, judging from the densitometry experiments, is reminiscent of a glasslike transition.

According to Fig. 2, curve 3, the high temperature transition affects also the structure of the mixed vesicle. The  $D_1$  vs.  $T$  plots exhibit a break around the transition temperature,  $T_g^*$ , of the pure polymerized lipid (butadiene). The horizontal deflection at  $T_s < T < T_g^*$  suggests that at the transition  $T_g^*$  of the polymer, lateral phase separation into rigid regions of the polymer gel and into fluid DMPC-rich regions sets in. With decreasing temperature the DMPC-rich phase is expected to become poorer in polymer. This would explain the finding that  $D_1$  is constant as the temperature drops from  $T_g^*$  to  $T_s$ . At the lower temperature limit,  $D_1$  drops rather steeply indicating that it now corresponds to the solidus line with all fluid domains solidified. This point of deflection is considerably higher than the melting transition temperature of pure DMPC. A possible explanation for this is, that small oligomer fragments still exist, and are dissolved in the fluid, DMPC-rich regions.

Further evidence for lateral phase separation at  $T < T_g^*$  is provided by Fig. 5, which shows micrographs of vesicles of a 1:1 mixture of DMPC and butadiene lipid (Scheme I) polymerized at  $T = 40^\circ\text{C}$ , which has been doped with 0.1 mol % fluorescence probe diO<sub>18</sub>. At high temperature ( $T > T_g^*$ ) the vesicles show a homogeneous distribution of the fluorescence emission. Immediately after cooling down to  $T = T_g$ , bright patches of  $\sim 5\ \mu\text{m}$  diam appear. Simultaneously the vesicles shrink and the patches grow into spikes that form fine tubelike protrusions at their tips (Fig. 5 b). The excess volume of the vesicle interior caused by the

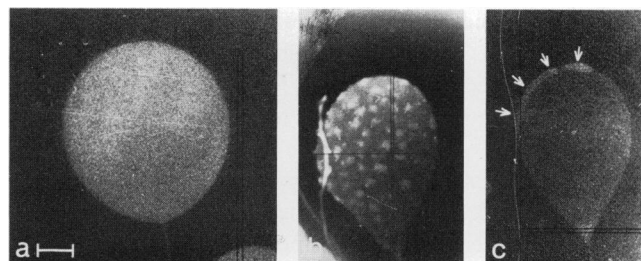


FIGURE 5 Photomicrograph of giant vesicles of 1:1 mixture of polymerized lipid (butadiene) and DMPC doped with diO<sub>18</sub>. (a)  $T = 40^\circ\text{C}$ , that is above the glasslike transition of polymerized butadiene lipid. (b) Same vesicle immediately after lowering the temperature below phase change of butadiene lipid. Note the strongly fluorescent tubelike protuberans coming out of the tips of the spikes. (c) Vesicle observed some minutes after lowering the temperature when bright patches have merged forming a cap (arrows). The size of the bar is  $10\ \mu\text{m}$ .

shrinking is pressed out through these tubes, whereby some of the lipid may be lost due to microvesicle formation. After this process the protrusions vanish leaving the small patches. These patches swim in the plane of the membrane.

They merge within  $\sim 200\ \text{s}$  forming strongly fluorescent caps. This capping process shown in Fig. 5 c obviously minimizes the surface energy of the vesicle. We assume that the patches are formed by polymerized lipid, while the bulk of the bilayer consists of DMPC containing some of the polymer. Evidence for this is provided by the finding of a high coefficient of lateral diffusion ( $D_1 = 8 \cdot 10^{-8}\ \text{cm}^2/\text{s}$  of Fig. 2, curve 3). The latter was measured in the region between the patches. After the formation of the patches,  $D_1$  is time independent.

We believe that the physical properties of the mixed polymer/monomer bilayer exhibit some analogies to the plasma membranes of cells. In the latter case the bilayer couples to the polymer network of the cytoskeleton via integral proteins (16), while in our case the polymerization occurs in the bilayer itself. In both systems the cap formation process seems to be initiated by a localized cross-linking of membrane components, which leads to a local deformation of the membrane. The system may thus become unstable and the cap formation sets in. The merging of the domains may well be a passive process that is driven by a long-range elastic interaction between the patches (17). It is generally assumed that cap formation is an energy requiring process that involves contractile microfilament activity (18). However, our experiments suggest that the energy consuming process of cap formation in plasma membranes could be limited to the initiation of the cross-linking process. In this case the energy liberated upon binding of ligands to the receptor could be sufficient. It appears that the coupling of the fluid bilayer to a polymerizable system may allow the amplification of a local disturbance (such as ligand-receptor binding) into a macroscopic reorganization of the whole membrane.

A remarkable observation is the rather small reduction in the diffusion coefficient caused by the polymerization.

In the pure lipid (Scheme I) vesicle  $D_l$  decreases only by about a factor of five by polymerization. Moreover the fluorescence recovery is 100%. This shows that the long-range diffusion is only partially restricted and that no dye molecules are captured in the polymer network. This strongly suggests that the cross-linking extends at most over some 100 Å. An alternative pathway for transport between different sites of the membranes would be diffusion through the aqueous phase. However, this would involve three-dimensional diffusion, which is expected to be extremely ineffective.

This conclusion is consistent with the freeze fracture results shown in Fig. 4 according to which smooth surfaces are observed both above and below the transition temperature of the pure components. The same observation holds for all mixtures containing up to 50 mol % of DMPC. This provides strong evidence that DMPC and monomeric lipid (butadiene; Scheme I) exhibit miscibility both in the fluid state (above the liquidus) and in the completely solidified state (below the solidus line). All experiences gained hitherto with at least 10 different lipid mixtures containing DMPC show that in the  $P'_\beta$ -phase of the latter, a corrugated surface profile results if the system exhibits immiscibility. Further evidence for this conclusion is provided by the sharp drop of the  $D_l$  vs. temperature curve for the DMPC/lipid (butadiene) mixture in the unpolymerized state.

Polymerization leads to the segregation into a DMPC-rich phase and the polymer. Both phases form elongated domains that are arranged alternately in parallel stripes. The same fingerprint-like pattern is obtained both if the polymerization is performed in the solid state or if the vesicle is frozen after performing the cross-linking in the fluid state. The wavelength of the corrugated pattern is  $\sim 400$  Å in both cases. The stripes are formed during freezing due to lateral phase separation taking place while the coexisting region of fluid, DMPC-rich and solidified (polymerized) butadiene lipid-rich phases, is traversed upon freezing. The finding that the same type of texture is observed if the order of the freezing and the polymerization process is exchanged may be understood by assuming that only small polymers are formed. The upper limit of the aggregation number,  $N$ , of the polymer is determined by the wavelength. One estimates a value of  $N \leq 100$  monomers/macromolecule. This small aggregation number could also explain the finding that even polymerized giant vesicles can be fused by the dielectric breakdown method (9).

Fig. 6 shows how  $D_l$  depends on the dilution of the lipid (Scheme I) with DMPC. In the unpolymerized state one obtains a linear relationship corresponding to ideal behavior. In the polymerized state one observes a clear deviation from ideality (dashed curve). It is interesting to compare our results with a recent theory of lateral diffusion in heterogeneous bilayers by Saxton (19). This author showed how the lateral diffusion constant can be calcu-

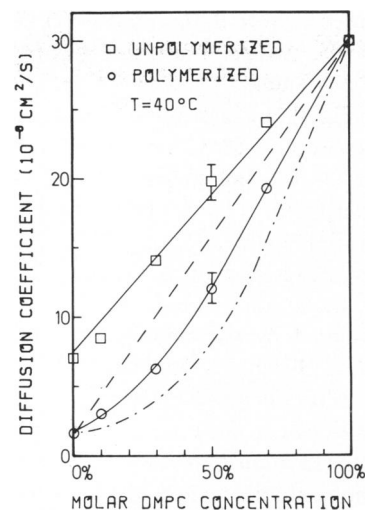


FIGURE 6 Variation of lateral diffusion coefficient in lipid (butadiene) bilayers upon dilution with DMPC. The dashed straight (---) line would correspond to an ideal mixture. The broken curve (— · —) is calculated for totally separated systems.

lated as a function of the area fractions of the separated phases by combining effective medium and percolation theory. The curve (— · —) in Fig. 6 has been calculated using Eq. 2 of reference 19 under the following two assumptions: (a) the system separates completely into patches of polymerized lipid (butadiene; Scheme I) and fluid DMPC, while the patch diameters are still small compared with the bleaching spot and (b) the fluorescence probe is uniformly partitioned between the two phases. The experimental and the theoretical curve deviate considerably. This discrepancy cannot be explained in terms of a nonuniform distribution of the dye, which would lead to an even larger deviation. According to reference 19 a nonuniform probe distribution would lead to an even stronger depression of the theoretical curve. Thus, we come to the conclusion (a) that our system behaves like a two-dimensional solution of a polymer and (b) that the size of the polymer is much smaller than the bleaching spot diameter. This agrees well with our freeze fracture result from which a diameter of the polymers of  $<400$  Å was estimated.

The value of the  $\text{diO}_{18}$  lateral diffusion coefficient in the fluid state of DMPC found here is larger by a factor of two than the corresponding value obtained with our previous apparatus (14) as well as that found by Wu et al. (20). However, it is by an order of magnitude higher than the diffusion coefficient reported by Fahey and Webb (21) for thin-walled DMPC vesicles. For that reason the value reported here has been measured very carefully several times to an accuracy of at least 10%. At present we do not have an explanation for this discrepancy. It shows, however, that at the present state of the FRAP-technique it is only possible to compare relative values of  $D_l$ .

Received for publication 2 March 1983 and in final form 29 August 1983.

## REFERENCES

1. Fendler, J. H. 1982. *Membrane Mimetic Chemistry*. First ed. John Wiley and Sons, Inc., New York. 113.
2. Gros, L., H. Ringsdorf, and H. Schupp. 1981. Polymeric antitumour agents on a molecular and on a cellular level. *Angew. Chem. Int. Ed. Engl.* 20:305-325.
3. Day, D., H. H. Hub, and H. Ringsdorf. 1979. Polymerization of mono- and bifunctional diacetylene derivatives in monolayers at the gas-water interface. *Isr. J. Chem.* 18:325-329.
4. Akimoto, A., K. Dorn, L. Gros, H. Ringsdorf, and H. Schupp. 1981. Polymer model membranes. *Angew. Chem. Int. Ed. Engl.* 20:90-91.
5. O'Brien, D. F., T. H. Whitesides, and R. T. Klingbiel. 1981. The photopolymerization of lipid-diacetylenes in bimolecular-layer membranes. *J. Polym. Sci.* 19:95-101.
6. Johnston, D. S., S. A. Sanghern, M. Pons, and D. Chapman. 1980. Phospholipid polymers — synthesis and spectral characteristics. *Biochim. Biophys. Acta.* 602:54-69.
7. Regen, S. L., B. Czech, and A. Singh. 1980. Polymerized vesicles. *J. Am. Chem. Soc.* 102:6638-6640.
8. Büschl, R., B. Hupfer, and H. Ringsdorf. 1982. Mixed monolayers and liposomes from natural and polymerizable lipids. *Makromol. Chem.* 3:589-596.
9. Büschl, R., H. Ringsdorf, and U. Zimmermann. 1982. Electric field-induced fusion of large liposomes from natural and polymerizable lipids. *FEBS (Fed. Eur. Biochem. Soc.) Lett.* 150:38-42.
10. de Gennes, P. G. 1979. *Scaling Concepts in Polymer Physics*. First ed. Cornell University Press, Ithaca, NY. 69.
11. Ringsdorf, H., and H. Schupp. 1981. Polymerization of substituted butadienes at the gas-water interface. *J. Macromol. Sci. Chem. A.* 15:701-715.
12. Ringsdorf, H., and H. Schupp. 1981. Polymerization of substituted butadienes at the gas-water interface. *J. Macromol. Sci. Chem. A.* 15:1015-1026.
13. Axelrod, D., D. E. Koppel, I. Schlessinger, E. Elson, and W. W. Webb. 1976. Mobility measurement by analysis of fluorescence photobleaching recovery kinetics. *Biophys. J.* 16:1055-1069.
14. Kapitza, H. G., and E. Sackmann. 1980. Local measurement of lateral motion in erythrocyte membranes by photobleaching technique. *Biochim. Biophys. Acta.* 595:56-64.
15. Peters, R., A. Brünner, and K. Schulten. 1981. Continuous fluorescence microphotolysis: a sensitive method for study of diffusion processes in single cells. *Proc. Natl. Acad. Sci. USA.* 78:926-966.
16. Branton, D., C. M. Cohen, and J. Tyler. 1981. Interaction of cytoskeletal proteins on the human erythrocyte membrane. *Cell.* 24:24-32.
17. Sackmann, E. 1979. On electrically-induced conformational changes and switching mechanisms in membranes. In *Light-induced Charge Separation in Biology and Chemistry*. H. Gerischer and I. I. Katz, editors. Berlin: Dahlem, Konferenzen. Verlag Chemie, Weinheim, New York. 259-285.
18. Hood, L. E., I. L. Weissmann, and W. B. Wood. 1978. *Immunology*. J. Hall, editor. Benjamin/Cummings Publishing Company Inc., Menlo Park, CA. 34.
19. Saxton, M. I. 1982. Lateral diffusion in an archipelago. *Biophys. J.* 39:165-173.
20. Wu, E. S., K. Jacobson, and D. Papahadiopoulos. 1977. Lateral diffusion in phospholipid multibilayers measured by fluorescence recovery after photobleaching. *Biochemistry.* 16:3936-3941.
21. Fanay, P.G., and W. W. Webb. 1978. Lateral diffusion in phospholipid bilayer membranes and multilamellar liquid crystals. *Biochemistry.* 17:3046-3053.